Theor Chem Acc (1998) 99:151–157

Theoretical
Chemistry Accounts

Regular article

Theoretical studies on the structure of $M^+BF_4^-$ ion pairs $M = Li^+, NH_4^+$: the role of electrostatics and electron correlation

C.H. Suresh, S.R. Gadre, S.P. Gejji

Department of Chemistry, University of Pune, Pune 411 007, India

Received: 9 September 1997 / Accepted: 5 November 1997

Abstract. A systematic investigation of the $M^+BF_4^-$ (M = Li or NH_4) ion-pair conformers has been carried out using an electrostatic docking model based on the molecular electrostatic potential topography of the free anion. This method provides a guideline for the subsequent ab initio molecular orbital calculations at the Hartree-Fock (HF) and second-order Møller-Plesset perturbation theory (MP2) levels. It has been demonstrated that the model presented here yields more than 75% of the HF interaction energy when Li^+ is the cation involved and more than 90% for the case of NH_4^+. Inclusion of MP2 correlation in the HF-optimized geometries leads to stationary point geometries with different numbers of imaginary frequencies and in some places where the energies of two adjacent conformers are very close, the energy rank order is altered. The HF lowest-energy minima for the $Li^+BF_4^-$ and $NH_4^+BF_4^-$ show a bidentate and tridentate coordinating cation, respectively, whereas at the MP2 level, this ordering is reversed.

Key words: Molecular electrostatic potential – Ab initio calculations

1 Introduction

Alkali metal or ammonium salts such as $LiBF_4$, $LiClO_4$ and NH_4SCN dissolved in polyether complexes, exhibit high ionic conductivity which depends on factors such as polymer segmental motion, cation-polymer interaction and the ionic association comprising of the formation of ion pairs or higher aggregates [1–2]. Among these factors, the ionic association could experimentally be monitored by infrared or Raman spectroscopy [3–6]. In recent years, theoretical work based on ab initio molecular orbital calculations has been employed to analyse the structural and spectral consequences of ion pairing [7–9]. Models based on electrostatic interactions have been used in the literature for predicting the structures of van der Waals (vdW) or hydrogen-bonded complexes [10–16]. Ion-pair complexes are of great interest and are frequently examined in the literature. Bonaccorsi et al. [17] have presented a comparison of electrostatic potentials in BH_4^- or AlH_4^- ions. The potential energy surface (PES) and deformation of XH_4^- in different structures of YXH_4 ($Y = Li^+$ and Na^+ ; X = B or Al) have also been discussed. Considering electrostatic interactions, polarization and covalent components of the anion-cation interaction, Baranov and Charkin [18] have analysed the stabilities of NF_4BF_4, NF_4AlF_4 and PF_4BF_4. They have pointed out [19] the importance of electron correlation in predicting the structure and stabilities of $Be(BH_4)_2$ and related systems. The PES for NH_4BH_4 has been reported by Baranov and Charkin [20]. Local minima of $M(BH_2)_2$ (M = Be, Mg and Ca) complexes have been located [21] within self-consistent field (SCF), MP2 and higher levels of theory. A discussion on how the extramolecular electrostatic potential acts as an indicator of chemical reactivity has been provided in an excellent review by Tomasi et al. [22]. They stressed the use of potential derived atomic charges for a first-order scanning of molecular conformations as well as non-covalent complexes. Further, the optimized geometries and the vibrational frequencies from the FTIR matrix isolation measurements of MBF_4 and $MAlF_4$ have been reported by Spoliti et al. [23]. In the present work, we focus on the structure and energetics of MBF_4 (M = Li and NH_4) ion-pair complexes where the electrostatic interactions are expected to be more predominant than those in vdW complexes. Specifically, a detailed analysis of the molecular electrostatic potential (MESP) topography [24] of the anion (BF_4^-) followed by an electrostatic docking of the cations at the critical point (CP) in the MESP have been carried out and used further for a systematic search of different ion-pair structures with the HF and MP2 levels of theory.

2 Methodology

Ab initio equilibrium geometries of BF_4^- and NH_4^+ were obtained by HF/6-31G (*d*, *p*), in the case of BF_4^-: 6-31G

Correspondence to: S.R. Gadre

(*d,p*) is identical to 6-31G (*d*), calculation using the GAMESS [25] package. The anionic wavefunction is used for the computation of the MESP topography employing the UNIPROP package [26]. Visualization of the MESP has been performed with a fortran code UNIVIS [26] written in our laboratory. A brief introductory description of the MESP and topography is provided below.

The MESP, $V(\mathbf{r})$, is the energy required to bring a unit positive charge from infinity to a point $\mathbf{r}$ which is given by

$$V(\mathbf{r}) = \sum_{A}^{N} \frac{Z_A}{|\mathbf{r} - \mathbf{R}_A|} - \int \frac{\rho(\mathbf{r}')d^3\mathbf{r}'}{|\mathbf{r} - \mathbf{r}'|} \tag{1}$$

where N is total number of nuclei in the molecule and Z_A is the charge of the nucleus located at $\mathbf{R}_A$. The two terms in the above equation denote the nuclear and electronic contributions, respectively. The topographical analysis [27] of $V(\mathbf{r})$ includes the location and identification of the CPs where the gradient of $V(\mathbf{r})$ vanishes. The rank of the CP is given by the number of non-zero eigenvalues of the Hessian matrix, A, the elements A_{ij} of which are defined as the second partial derivative of $V(\mathbf{r})$ with respect to x_i and x_j at the CP ($\mathbf{r} = \mathbf{r}_c$). A CP is characterized in terms of an ordered pair (R, σ) where R is the rank of the matrix A and σ denotes the signature, i.e. an algebraic sum of the signs of these eigenvalues. A non-degenerate CP of rank 3 corresponds to a maximum for $\sigma = -3$, a saddle point for $\sigma = -1$ or $+1$ and a local minimum for $\sigma = +3$. These local minima or saddles in the MESP of the anion are considered as the probable interaction sites for the cation.

A quick, yet fairly good, estimation of the interaction energy for a cation-anion pair is made by evaluating the integral

$$E_{\text{int}}^{\text{dock}} = \int V_A(\mathbf{r})\rho_c(\mathbf{r})d^3\mathbf{r} \tag{2}$$

where V_A ($\mathbf{r}$) refers to the electrostatic potential of the anion and $\rho_c(\mathbf{r})$ defines the charge density of the cation at that site. Thus, the cation coordination, predominantly electrostatic in nature, may be understood in terms of a lock and key mechanism wherein the cation (the key) tries to recognize the most negative MESP regions of the anion (the lock). An electrostatic docking model (cf. Eq. 2) is proposed. This includes identification of the different CPs of the anionic MESP surface. This has been followed by defining the size of the anion by assigning the radii to each atom using the MESP CPs. Ionic radii are used for the cations [28]. These radii limit the distance of closest approach of the two ions. Since an anion will show different negative MESP CPs all around the nuclear framework, the docking model will engender various possibilities for the cation coordination providing an estimate for the interaction energies through the minimization of the integral in Eq. (2). During this minimization process, the internal coordinates of the anion and those of the cation are kept intact. The model-predicted geometries may thus be used for a systematic search for the ion-pair geometries at higher level of theory. In the present work, the model geometries are first optimized at the HF level using the 6-31G (*d, p*) basis set and the interaction energies are calculated. The effect of electron correlation is included via the MP2 theory.

3 Results and discussion

The HF/6-31G (*d*) MESP topography of the tetrahedral tetrafluoroborate anion shows the following rich topographical features. In all there are 38 negative valued CPs which can be grouped into 5 different degenerate sets (cf. Table 1). These include (3, +1) CPs at the centre of each face of the anionic tetrahedron (denoted by p5), (3,−1) CPs located at the corners (denoted by p4), and (3,−1) CPs at the edges of the tetrahedron (denoted by p3). Each (3,−1) CP of a fluorine at the corner of the tetrahedron is encircled by two triplets of (3, +3) and (3, +1) CPs. A top view of the anion along a corner shows that the (3, +3) triplet is eclipsing the rest of the fluorines whereas the (3, +1) triplet has a staggered arrangement. The (3, +3) and (3, +1) triplets are denoted by p1 and p2, respectively. This arrangement of MESP CPs for BF_4^- is shown in Fig. 1. Only representative CPs are depicted in this figure and some symmetry-related CPs are not shown. For assesing the role of correlation on MESP topography, the latter was also computed at the MP2/6-31G(d) level. These results shown in Table 1, however indicate that there is no substantial difference in the HF and MP2 -level topography: the corresponding MESP values at the CP's differ by not more than 4 per cent and the distances of CP's from the nearest atom show a maximum change of 0.06 Å only. However, since there is no qualitative change between HF and MP2-level MESP distribution, the former is used in all the discussion that follows. The distances of these CPs from the centre of the tetrahedron

Table 1. Molecular electrostatic potential (*MESP*) topography of BF_4^- at Hartree-Fock (*HF*)/6-31G* and second-order Møller-Plesset (*MP2*)/6-31G* levels. See Fig. 1 for details

MESP CP	Type of CP	MESP value (a.u.)		Distance from boron (Å)		Distance from fluorine (Å)	
		HF	MP2	HF	MP2	HF	MP2
p1	(3, +3)	−0.2475	−0.2454	2.00	1.92	1.14	1.18
p2	(3, +1)	−0.2451	−0.2421	2.06	2.01	1.12	1.15
p3	(3, +1)	−0.2374	−0.2405	1.76	1.74	1.48	1.48
p4	(3, −1)	−0.2276	−0.2188	2.53	2.58	1.14	1.16
p5	(3, −1)	−0.2048	−0.2110	1.82	1.78	1.89	1.87

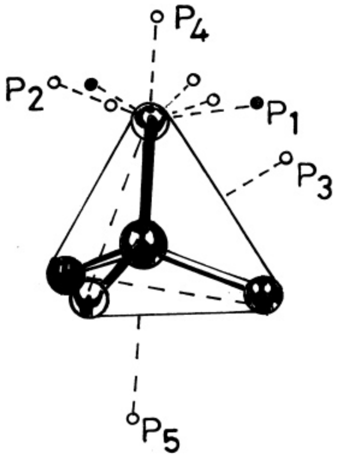

Fig. 1. Molecular electrostatic potential (MESP) topography of the BF_4^- ion showing some of the critical points (CPs) defined as p1, p2, p3, p4 and p5

(i.e. from the boron atom) and the nearest fluorine along with the corresponding MESP values are given in Table 1. The distance of p3 from the nearest fluorine (i.e. 1.48 Å) and of p5 from boron (1.82 Å) are taken as the radii for fluorine and boron, respectively. Pauling's [28] ionic radii, 0.60 Å for Li^+ and 1.48 Å for NH_4^+, are used for the cations in these ion-pair systems. MESP values at these CPs are ordered as: $p5 > p4 > p3 > p2 > p1$. This suggests that a cation is attracted towards these CPs with varying degrees of strength of interaction.

Electrostatic docking as described Sect. 2, was carried out for the Li^+ and NH_4^+ cations with the BF_4^- anion. For Li^+ 5 different docked geometries (A1–A5) were derived as shown in Figs. 2 and 10 (B1–B10) for NH_4^+ as given in Fig. 3. A greater number of possibilities are intuitively expected for NH_4^+ due to the non-spherical character of the charge density (in accordance with this spheres of radii, 1.00 Å for nitrogen and 0.48 Å for hydrogen consistent with the ionic radius of 1.48 Å for the NH_4^+ ion, are used for the electrostatic docking). The dotted lines in the figure show how the cation is bound to the BF_4^- anion via the nearby CPs. It is found that at the docked geometries the maximum gradient norms are typically 10^{-2} au, and a full ab initio optimization starting from these structures at the HF/6-31G (*d*, *p*) level converged quickly to stationary states (typically 13–18 optimization cycles with GAMESS). This indicates that the docked structures were in the vicinity of the HF stationary points. The interaction energies for the ion pairs (calculated as the difference between the total energy of the ion pair and the sum of the total energies of the free ions) obtained with the docking ($E_{\text{int}}^{\text{dock}}$) (purely electrostatic) and the HF optimization ($E_{\text{int}}^{\text{HF}}$) are presented in Tables 2 and Table 3, respectively. The present docking model reproduces ~76% and ~95% of the total HF interaction energy ($E_{\text{int}}^{\text{HF}}$) for the $Li^+BF_4^-$ and $NH_4^+BF_4^-$ ion pairs, respectively.

Geometries derived from the model and those from the HF calculations are compared in Table 4 and Table 5 for the $Li^+BF_4^-$ and $NH_4^+BF_4^-$ ion pairs, respectively. The docked geometries of $Li^+BF_4^-$ labelled as A1–A5 and those of $NH_4^+BF_4^-$ represented as B1–B10 are shown in Figs. 2 and 3, respectively. Since A1 and A2 converge to the same optimized structure in the HF calculations the A2 conformer is not included in Table 4. Except for the A1 and A2 conformers, the orientations of the cation and the anion in the HF equilibrium structures (A3–A5 and B1–B10) were close to the respective docked ones. The B-F bonds with the coordinated fluorines are longer than those in the free anion. Except in a few cases (A4 and B6) the change in the B-F bond length is typically ~0.05 Å. In general, the interionic bonds show a deviation of ~0.30 Å (A5, B4 and B6 are exceptions) when compared with the docked geometries. The F-B-F angles vary from 1° to 10° as compared to those in the free anion. A comparison of the different H-N-H, Li-F-B, N-F-B and H-N-F bond angles and dihedral angles are generally in good agreement with those of the model geometries. The general agreement between the MESP-

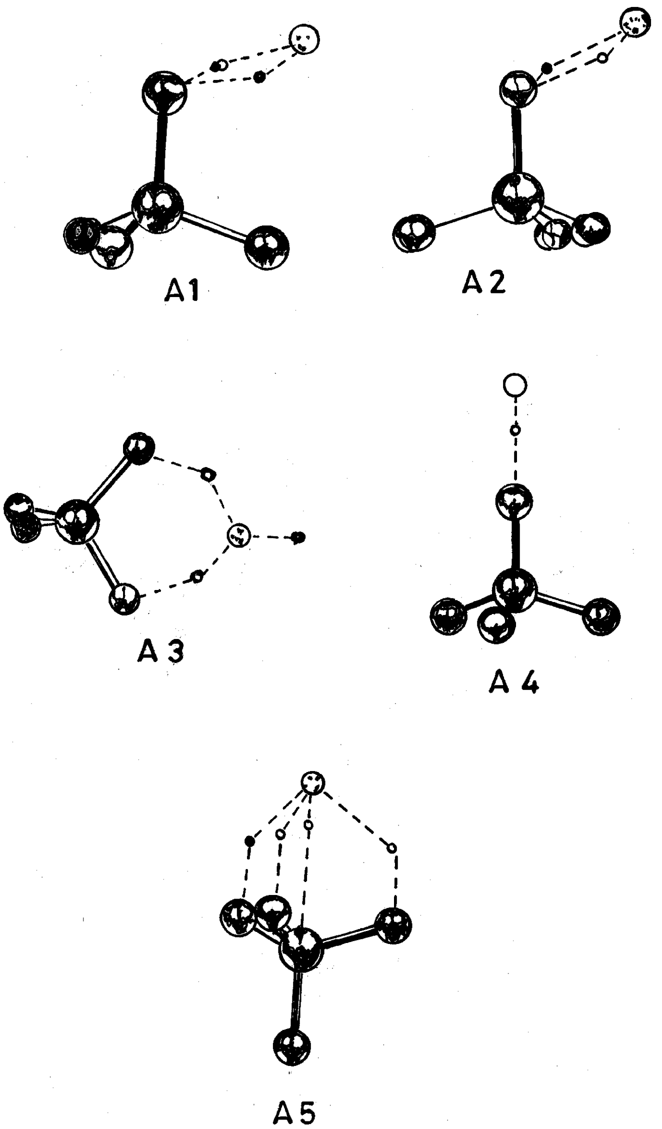

Fig. 2. HF/6-31G (*d*) electrostatic docked geometries for the $BF_4^-Li^+$ ionpair. CPs are shown as *small dots* and their connections with the atoms of the cation and the anion are represented by *dotted lines*

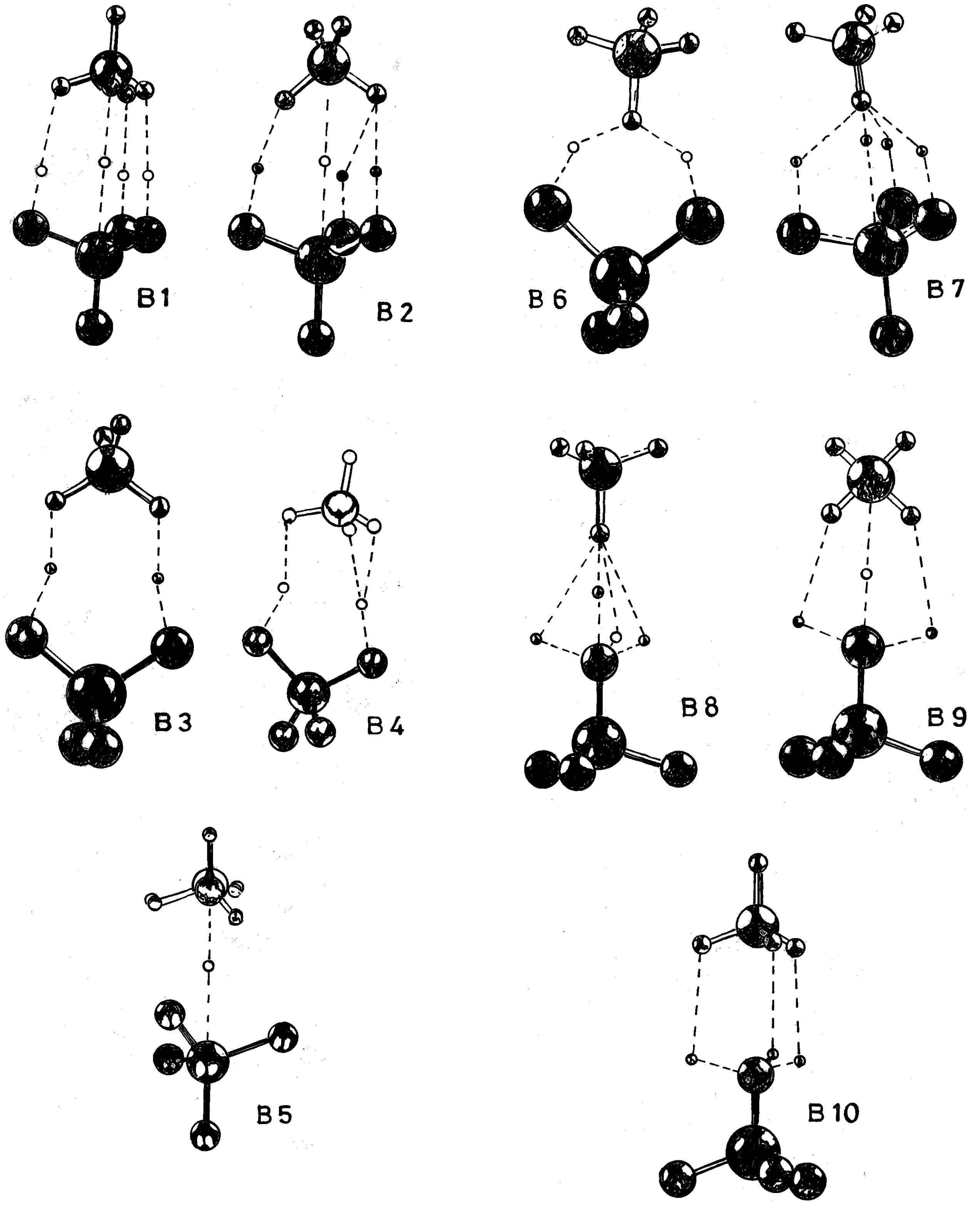

Fig. 3a, b. HF/6-31G (*d*, *p*) electrostatic docked geometries for the $BF_4^-NH_4^+$ ionpair. CPs are shown as *small dots* and their connections with the atoms of the cation and the anion are represented by *dotted lines*

predicted geometries and the HF geometries thus implies that the MESP topography of an anion plays a central role in directing the cation towards a specific region of the anion. The model-predicted interaction energies which agree qualitatively with the HF ones exhibit the following trend of stability: A4 > A2 > A1 > A5 > A3 (cf. Table 2). In the case of $NH_4^+BF_4^-$ ionpairs the interaction energies obtained from the model as well as

Table 2. Energetics of $BF_4^-Li^+$ ion-pair conformers at the electrostatic docked, HF and MP2 optimized positions using the 6-31G* basis set (all values are in a.u.)

Docking Structure	E_{int}^{dock}	HF[a]		MP2[a]	
		Total SCF Energy (Nimag)[b]	E_{int}^{HF}	Total MP2 Energy(NImag)[b]	E_{int}^{MP2}
A1	−0.185	−430.20238 (1)	−0.2417	−431.00309 (0)[d]	−0.257
A2	−0.183	−430.20238 (1)[c]	−0.2417	−431.00309 (0)[d]	−0.257
A3	−0.192	−430.20682 (0)	−0.2461	−431.00295 (0)	−0.257
A4	−0.164	−430.17534 (2)	−0.2147	−430.96744 (2)	−0.222
A5	−0.188	−430.20303 (0)	−0.2423	−431.00309 (0)[d]	−0.257

[a] The HF energies of free BF_4^- and Li^+ are −422.72515 and −7.23554 a.u. respectively, their sum being −429.96069 a.u. The corresponding MP2 values are −423.50968, −7.23594 and −430.74562 a.u

[b] Number of imaginary frequencies

[c] This transition structure (TS) is identical to that obtained from A1

[d] These three structures are identical

Table 3. Energetics of BF_4^- NH_4^+ ion-pair conformers at the electrostatic docked, HF and MP2 optimized positions using the 6-31G** basis-set (all energies are in a.u.)

Docking Struc-ture	E_{int}^{dock}	HF[a]		MP2[a]	
		Total SCF energy (NImag)[b]	E_{int}^{HF}	Total MP2 energy (NImag)[b]	E_{int}^{MP2}
B1	−0.177	−479.45302 (0)	−0.182	−480.44283 (2)	−0.196
B2	−0.164	−479.44990 (1)	−0.179	−480.44284 (0)	−0.196[c]
B3	−0.164	−479.44871 (1)	−0.178	−480.44284 (0)	−0.196[c]
B4	−0.170	−479.44730 (1)	−0.177	−480.43664 (3)	−0.189
B5	−0.171	−479.44672 (1)	−0.176	−480.43364 (3)	−0.186
B6	−0.162	−479.44072 (3)	−0.170	−480.42356 (3)	−0.180
B7	−0.151	−479.43732 (2)	−0.167	−480.41567 (3)	−0.176
B8	−0.130	−479.42901 (2)	−0.158	−480.42772 (3)	−0.168
B9	−0.145	−479.42181 (3)	−0.151	−480.40525 (3)	−0.158
B10	−0.141	−479.42172 (4)	−0.151	−480.40388 (3)	−0.157

[a] The HF energies of free BF_4^- and NH_4^+ are −422.72515 and −56.54553 a.u., respectively, their sum being −479.27068 a.u. The corresponding MP2 values are −423.50968, −56.73765 and −480.24733 a.u

[b] Number of imaginary frequencies

[c] These two structures are identical.

Table 4. Geometrical parameters of the docked and corresponding HF conformers of $BF_4^-Li^+$ ion pairs in Å. The *starred values* represent the bonds involving atoms connected to lithium. Values in *parentheses* stand for the docked ones. In the free anion, the B-F bond length is 1.39 Å and the F-B-F bond angle is 109.5°

	A1	A3	A4	A5
B-F1	1.44*	1.46*	1.56*	1.32
B-F2	1.38	1.34	1.35	1.42*
B-F3	1.44*	1.46*	1.35	1.42*
B-F4	1.33	1.34	1.35	1.42*
Li-F*	1.83 (2.08)	1.76 (2.08)	1.63 (2.08)	1.92 (2.36)
F2-B-F1	104.3	109.9	103.9	115.9
F3-B-F1	100.5	98.9	103.9	115.9
F4-B-F1	114.3	109.9	103.9	115.9
Li-F-B	79.8 (117.5)	91.5 (92.1)	180.0 (180.0)	74.3 (75.6)

the HF-optimized values (E_{int}^{HF}) for the B1–B5 conformers are found to be higher than the ones for B6–B10 conformers. Making yet finer distinctions for the conformers that are close in energy becomes rather difficult using the present simple electrostatic-based model.

The HF structure obtained from A1 (which is the same as the one from A2) was characterized as a transition state (TS) (1 imaginary frequency) and is slightly different from either of A1 or A2 docked geometries. Unlike the docked structures, in the corresponding TS, lithium is equidistant from the two oxygens. Ion-pair conformers derived from A3 and A5 are local minima (all frequencies are real) whereas A4 represents a maximum (two imaginary frequencies). For the $NH_4^+BF_4^-$ conformers, the B1 structure leads to the only minimum B2, B3, B4, and B5 yield transition states and the remaining B6-B10 geometries represent higher order saddle points.

A transition state generally is expected to pass through a local minimum before reaching another transition state. Since in the present work, we have located four different TS and only one minimum, an attempt was made to locate other minima with the incorporation of the intrinsic reaction coordinate (IRC) calculation [29] starting with the transition state geometries as the initial guesses in the HF calculations. All these optimizations, however, failed to produce any other local minima except the one already found. Such

Table 5. Geometrical parameters of the docked and corresponding HF conformers of $BF_4^-NH_4^+$ ion pairs in Å. The *starred values* represents the bond distances involving atoms showing interionic bonds. Values in *parentheses* are those derived from the docking model. In the free tetrahedral ions the B-F and N-H bond lengths are 1.39 and 1.01 Å, respectively

	B1	B2	B3	B4	B5	B6	B7	B8	B9	B10
B-F1	1.34	1.43	1.35	1.46*	1.35	1.52*	1.36	1.35	1.47*	1.46*
B-F2	1.41*	1.40*	1.35	1.41*	1.41*	1.36	1.36	1.41*	1.37	1.37
B-F3	1.41*	1.40*	1.44*	1.35	1.41*	1.36	1.43*	1.41*	1.37	1.37
B-F4	1.41*	1.34	1.44*	1.35	1.41*	1.36	1.43*	1.41*	1.37	1.37
N-H1	1.00	1.03*	1.00	1.05*	1.00	1.09*	1.01	1.02*	1.01	1.00
N-H2	1.02*	1.01*	1.00	1.00	1.01*	1.01	1.03*	1.01	1.01	1.01*
N-H3	1.02*	1.00	1.03*	1.01*	1.01*	1.01	1.01	1.01	1.02*	1.01*
N-H4	1.02*	1.00	1.03*	1.01*	1.01*	1.01	1.01	1.01	1.02*	1.01*
H*-F*[a]	1.91	2.11	1.67	1.52	2.22	1.33	1.76	1.97	1.90	2.13
	(2.07)	(2.33)	(1.95)	(1.96)	(2.35)	(1.95)	(1.95)	(1.95)	(2.08)	(2.36)
<NFB	82.8	82.9	101.0	63.6	83.2	180.0	103.5	86.1	179.6	180.0
	(80.5)	(87.5)	(100.8)	(96.8)	(80.5)	(180.0)	(106.0)	(96.6)	(179.5)	(180.0)
<H1NF1	150.3	17.7	120.3	177.4	150.4	0.0	111.1	27.3	120.2	180.0
	(151.0)	(27.5)	(124.7)	(153.8)	(151.0)	(0.0)	(109.9)	(13.0)	(120.5)	(180.0)
<H2NF1	36.5	85.5	120.0	69.5	55.4	109.5	25.3	119.6	128.8	66.5
	(41.6)	(82.0)	(118.7)	(59.5)	(58.7)	(109.5)	(19.2)	(117.1)	(130.0)	(70.5)
<H3NF1	83.0	118.3	76.4	69.5	96.5	109.5	126.9	80.8	50.1	66.5
	(83.4)	(120.9)	(79.2)	(59.5)	(99.5)	(109.0)	(123.5)	(96.6)	(54.9)	(70.5)
<H4NF1	83.0	118.1	23.6	113.8	55.4	109.5	84.4	119.6	50.1	66.5
	(84.4)	(120.9)	(30.5)	106.0	(58.7)	(109.5)	(90.6)	(113.8)	(54.9)	(70.5)
<H-N-H[b]	113.7	110.8	111.5	113.8	113.1	109.5	110.1	110.8	110.9	113.5
	104.9	103.2	100.0	106.0	105.6	109.4	108.1	108.1	100.1	105.1

[a] H*-F denotes the shortest H-F distances.

[b] Largest and smallest angles. The other angles are not reported.

bifurcations of the PES, have been reported earlier in the literature [30, 31]. In order to study the electron correlation effects in these ion-pair systems, full MP2 optimizations were performed. The electronic energies of different conformers thus obtained and the number of imaginary frequencies are reported for $Li^+BF_4^-$ion-pair in Table 3. For this case, the most stable conformer in the MP2 calculations was a tridentate coordinated structure. The transition state in the HF theory, however, led to this tridentate minimum. Other HF structures retained their characteristics of coordination at the MP2 level of theory. Unlike the $Li^+BF_4^-$ ion-pairs, more striking differences are noticed for NH_4^- BF_4^- as reported in Table 4. Here the bi-dentate structure (which was a TS at HF level) is emerged as the lowest minimum and the tri-dentate coordinated structure (which was the minimum at HF level) turns out to be a maximum on the MP2 PES. The remaining TS and other saddle point geometries at the HF level led to the higher order saddle points retaining the same orientations of the anion and the cation. A geometry similar to B2 was not identified in the MP2 calculations. This conformer finally converges to a structure similar to the one obtained from B3.

A comparison of the HF-SCF energies at the MP2 geometries with the MP2 ones shows that the alterations in the energy rank order are solely brought about through the MP2 correlation (cf. Table 3). For example, the rank order for A2 and A3 at the MP2 level is exactly the reverse of the one seen from the SCF energy at the MP2 geometry (this order is the same as the one obtained from HF theory). The observation is similar for the B1 and B3 geometries.

A comparison of the bond lengths of the HF and MP2 ion-pair geometries reveals the following features. For $Li^+BF_4^-$ ion-pairs the B-F bonds as well as interionic bonds (coordinated Li-F bonds) are ~0.02 and 0.01 Å longer in the MP2-level calculations. In contrast to this, all $NH_4^+BF_4^-$ conformers show an elongation of the B-F and N-H bonds (maximum upto 0.06 and 0.07 Å, respectively) and a shortening of interionic hydrogen bonds ranging from 0.05 to 0.13 Å.

4 Conclusions

The present MESP topography-based model offers a systematic approach for analysing different ion-pair conformers. Geometries and the electrostatic interaction energies obtained from such a model provide fairly good estimates for the HF interaction energies. Although the ion-pair geometries show marked differences in the nature of the stationary points on the PES for the HF and MP2 levels in terms of the number of imaginary frequencies, their energy rank order is not much affected. Some subtle changes, however, may be due to the rather flat nature of the corresponding PES. In summary electrostatic investigations are seen to provide excellent starting points for a further detailed quantum-chemical investigation. This approach is being further explored for a variety of ion-pairs in our laboratory.

Acknowledgements. S.R.G. is grateful to the Council of Scientific and Industrial Research (CSIR), New Delhi for sponsoring a research project [01 (1430)/96/EMR-II]. C.H.S. thanks CSIR, New Delhi for the award of a senior research fellowship. S.P.G. acknowledges support from the University Grants Commission (UGC) in the form of a minor research project.

References

1. MacCallum JR, Vincent CA (eds) (1987) Polymer electrolyte reviews 1. Elsevier, London, Chap. 2
2. See, for example (a) Frech R, Huang W (1994) Solid state ionics 72:103; (b) Huang W, Frech R (1994) Polymer 35:235
3. James DW, Mayes RE (1984) J Phys Chem 88:637
4. Addison CC, Amos DW, Sutton D (1968) J Chem Soc 2285
5. Burger K (1983) Studies in analytical chemistry 6: solvation and complex formation reactions in non-aqueous solvents. Elsevier, Amsterdam
6. Papke BL, Ratner MA, Shriver DF (1982) J Electrochem Soc 129:1694
7. Francisco JS, Williams IH (1990) J Phys Chem 94:8522
8. Francisco JS, Williams IH (1992) J Phys Chem 96:7567
9. Klassen B, Aroca R, Nazri A (1996) J Phys Chem 100:9334
10. Gadre SR, Bhadane PK, Pundlik SS, Pingale SS (1996) In: Murray JS, Sen K (eds) Molecular electrostatic potentials: concepts and applications. Elsevier, Amsterdam, Chap. 5, pp 219
11. See, for example, (a) Legon AC, Millen DJ (1987) Chem Soc Rev 16:467; (b) Dykstra CE (1989) J Am Chem Soc 111:6168; (c) Alhambra C, Luque FJ, Orozco M (1995) J Phys Chem 99:3084
12. Buckingham AD, Fowler PW (1983) J Chem Phys 79:6426
13. Buckingham AD, Fowler PW (1985) Can J Chem 63:2018
14. Politzer P, Truhlar DG (1981) Chemical applications of atomic and molecular electrostatic potentials. Plenum, New York
15. Bonaccorsi R, Scrocco E, Tomasi J (1970) J Chem Phys 52:5270
16. Naray-Szabo G, Ferenczy GC (1995) Chem Rev 4:829
17. Bonaccorsi R, Scrocco E, Tomasi J (1979) Theor Chim Acta 52:113
18. Baranov LY, Charkin OP (1990) Zh Neorg Khim 35:2899
19. Baranov LY, Charkin OP (1989) Zh Neorg Khim 34:1928
20. Baranov LY, Charkin OP (1989) Zh Strukt Khim 30:27
21. Bonaccorsi R, Charkin OP, Tomasi J (1991) Inorg Chem 30:2964
22. Tomasi J, Bonaccorsi R, Cammi R (1991) In: Maksic ZB (ed) Theoretical models of chemical bonding, vol 4. Springer, Berlin Heidelberg New York, p 228
23. Spoliti M, Sanna N, Martino VD (1992) J Mol Struct (Theochem) 90:83
24. (a) Gadre SR, Kulkarni SA, Shrivastava IH (1992) J Chem Phys 96:5253; (b) Gadre SR, Kölmel C, Shrivastava IH (1992) Inorg Chem 31:2281; (c) Gadre SR, Pathak RK (1990) J Chem Phys 93:1770
25. GAMESS version 22. Schmidt MW, Baldridge KK, Boatz JA, Elbert ST, Gordon MS, Jensen JH, Koseki S, Matsunaga M, Nguyen KA, Su SJ, Windus TL, Dupuis M, Montgomery JA 1995 J Comp Chem 14:1347
26. The package UNIPROP was developed by Gadre SR and coworkers, Department of Chemistry, University of Pune, Pune 411 007, India; The package UNIVIS (a PC-based molecular property visualization package) was developed by Limaye AC, Inamdar PV, Dattawadkar SM, Gadre SR (1996) J Mol Graph 14:19
27. Bader RFW (1990) Atoms in molecules: a quantum theory. Clarendon, Oxford
28. Pauling L (1942) The nature of the chemical bond. Cornell University, Ithaca, New York
29. Gonzales C, Schlegel HB (1990) J Phys Chem 94:5523 Gonzales C, Schlegel HB (1991) J Chem Phys 95:5853
30. Kapp J, Schreiner PR, Schleyer PvR (1996) J Am Chem Soc 118:12154
31. Heidrich D, Kliesch W, Quapp W (1991) In: Properties of Chemically Interesting Potential Energy Surfaces, Springer-Verlag, Berlin p 117